Proceedings of HT2005
2005 ASME Summer Heat Transfer Conference
July 17-22, 2005, San Francisco, California, USA

HT2005-72777

CONFINEMENT OF FREEZING FRONT BY LASER IRRADIATION DURING CRYOSURGERY

Ricardo Romero-Méndez [a,b], Kevin Chu [a], Henry Vu [a], Walfre Franco [a], Guillermo Aguilar [a]

[a] Department of Mechanical Engineering, University of California, Riverside, CA 92521
[b] School of Engineering, Universidad Autónoma de San Luis Potosí, SLP, México 78290

ABSTRACT

A new methodology to control the freezing front propagation during cryosurgical procedures is studied through the use of numerical techniques. Laser irradiation of a target tissue is explored as a new methodology for localizing heat generation and, thus, confining more accurately the desired cryoinjury region and to protect a thicker superficial layer of tissue. In addition to the irradiation of laser energy, the use of dyes is proposed as a means of localizing heat absorption and increasing the thickness of the protected region.

A 2D finite volume numerical code based on the enthalpy method was developed to model the freezing process during cryoprobe cooling of a volume of tissue, while heating was applied to the external boundary protecting the superficial layer of tissue. Laser irradiation was modeled with Beer's Law, and the energy absorption, which is proportional to the intensity, was taken as a source term in the energy equation. The thermophysical properties of the tissue are modeled as temperature dependent properties of water. Temperature contours resulting from a) constant temperature heating b) and regulated laser irradiation heating of tissue indicate that the latter methodology may be more effective in limiting cryoinjury to a predefined region. Additionally, if dyes are used, the protected area increases in thickness. The most dramatic differences between the two methodologies occur when the cryoprobe is placed near the surface, the effective attenuation coefficient of the material is low, and dyes are injected into the tissue to promote localized absorption of laser irradiated energy.

NOMENCLATURE

Bi	Biot number, $Bi=hy_o/k_s$
C	specific heat (J kg^{-1} K^{-1})
d	position in the y direction (m)
E	enthalpy (J)
h	heat transfer coefficient (W m^{-2} K^{-1})
H	depth (m)
$I(y)$	laser irradiance at a distance y (W m^{-2})
I_o	laser output irradiance (W m^{-2})
k	thermal conductivity (W m^{-1} K^{-1})
L	latent heat of fusion (J kg^{-1})
q	heat flux (W m^{-2})
Q	heat source, (W m^{-3})
St	Stefan number
t	time (s)
T	temperature ($^\circ$C)
T_∞	temperature of surroundings ($^\circ$C)
x	coordinate tangential to the surface (m)
y	coordinate normal to the surface (m)
y_o	side of square prism
y^*	dimensionless coordinate, $y^*=y/y_o$

Greek letters

α	effective attenuation coefficient (m^{-1})
β	ratio of liquid to solid thermal diffusivities
δ	thickness of dye layer (m)
ε	laser protection effectiveness coefficient
κ	ratio of liquid to solid conductivities
λ	interface location
ρ	density (kg m^{-3})

τ dimensionless time, $\tau=2k_s t/\rho_s C_s y_o$

Θ dimensionless temperature, $\Theta=(T-T_\infty)/(T_m-T_\infty)$

Subscripts

cryo	cryoprobe
d	dye
i	initial value
l	liquid phase
lethal	lethal value
m	phase change
s	solid phase
w	heating wall

INTRODUCTION

Cryoablation of tissue using direct placement of cryoprobes within the tissue is a technique that has been gaining acceptance as a procedure for the treatment of internal cancer. The technique was first proposed by Arnott [1], but the first cryosurgical device for the treatment of internal tissues was presented by Cooper and Lee [2] in 1961. The technique compares favorably with other techniques, such as radical surgery and irradiation of tissue, because of the less traumatic procedure which reduces the blood loss and hospitalization times, which makes it the most recommended procedure for patients that are too ill or too old to undergo major surgery or for those with a very localized disease. Although used for various tissue malignancies, the most successful application of cryosurgery has been for the eradication of prostatic cancer. In 1993, Onik *et al.* [3], presented preliminary results indicating that ultrasound-guided prostate cryosurgery may be an effective treatment for prostate cancer with minimal associated morbidity.

During prostate cancer cryosurgery metal freezing probes, called cryoprobes, are inserted into the tissue and cryogen flows through the probes which are in direct contact with the tissue. These cryoprobes have experienced technological improvements in recent years, [4-6]. Mainly reduction in size and increased ability to control the freezing rate that make possible to increase the number of cryoprobes inserted into the tissue, and also increase the possibility of a successful cryosurgery. The freezing starts as the probes are turned on, and the individual iceballs of each probe end up coalescing to form a larger ice ball. The border of the iceball is monitored with the aid of transrectal ultrasound or by magnetic resonance imaging to make sure that the ice ball does not approach healthy tissue that, if damaged, would produce postoperative complications hindering the success of the cryosurgical procedure.

Among the most common postoperative complications, urinary rectal fistula is the most severe. During cryosurgery, the iceball is allowed to approach the rectal wall, but careful attention must be paid not to freeze the rectum. In order to kill all the unhealthy tissue, it may be necessary to allow the ice ball to get very near to the rectal wall without touching it.

Other complication that may be very severe is urethral sloughing. In order to avoid this complication, the urethral walls have to be protected from damage by impeding them to freeze during the procedure. With the appearance of the urethral warmer, first proposed by Cohen *et al.* [7], this complication has reduced significantly.

Although cryosurgery is a proven procedure for the eradication of prostatic cancer, the success of the procedure is still very dependent on the experience and good judgment of the surgeon, as he is the person who monitors the growth of the iceball and determines up to what point the ice ball is allowed to grow. The problem is twofold: the surgeon must be sure the complete unhealthy tissue has been lethally damaged but has to guarantee that the delicate urethra and rectum walls have been spared. Additionally, there is concern about the improvement of the monitoring procedure [8]. For the previously stated reasons, the surgeon may resort to treatment planning strategies, such as the optimal placement of cryoprobes to maximize ablation of the prostate while minimizing collateral damage. Efforts to improve the technique by modeling numerically the freezing and assessing the best placement for the cryoprobes have been done by researchers such as Baissalov *et al.* [9], Rewcastle *et al.* [10], and Rabin *et al.* [11].

In order to increase the likelihood of a successful cryosurgery, it would be desirable to devise effective ways to protect certain regions of tissue from being frozen without limiting so severely the application of the cryoprobe. If an artifact is created that guarantees that certain regions will never freeze, no matter how long the application of the cryoprobe is, a great progress may be achieved, as the cryosurgical procedure would become less dependent upon the good judgment of the surgeon. In this scenario is that this investigation proposes the use of laser irradiation as a means to guarantee the protection of superficial layers of tissue that may well represent the urethral or rectum walls. Other investigations, such as those of Rabin *et al* [12, 13], have proposed the use of so-called cryoheaters, but its effect is the protection of only a very superficial layer of tissue. The present investigation determines the effect achieved by laser irradiation and compares it to the protection achieved by other more conventional means of heating, such as warmers and cryoheaters.

PROBLEM DEFINITION

The problem studied herein assesses the advantages that regulated laser irradiation heating may have over the conventional constant temperature heating for the protection of tissue during cryosurgical procedures. The computational domain represented by Figure 1 consists of a rectangular body of depth H and width W. Inside this domain, a cryoprobe is placed at $x=0$ and $y=d$. The cryoprobe is represented as a rectangular block of dimensions H_{cryo} by W_{cryo}, whose surface is at T_{cryo}. The domain is assumed to be sufficiently deep so that the boundary, $y=H$, may be assumed to have a zero heat flux boundary condition. The sides of the block, $x=0$ and $x=W$, are assumed to be symmetry planes, as the system may be a part of a larger system having a row of cryoprobes separated by a distance $2W$ and placed all at the same depth. The boundary, $y=0$, is the heating boundary. Two different types of boundary conditions may be established, depending on the way the heat is being applied through the surface:

(a) Uniform constant temperature heating. The top surface is assumed to be in contact with another surface at T_w, and a perfect thermal contact exists between these surfaces, so the boundary condition is $T(x,0)=T_w$.

(b) Natural convection with air and laser irradiation through the surface. The top surface has natural convection

with surroundings at T_∞ and the associated convective heat transfer coefficient is h. The mathematical expression of the boundary condition is

$$-k\left.\frac{\partial T}{\partial y}\right|_{y=0} = h(T|_{y=0} - T_\infty), \qquad (1)$$

additionally, laser irradiation with a laser output irradiance I_o is being directed normally through this surface. Although there is not specification of the laser wavelength, a constant attenuation coefficient α is established for the material.

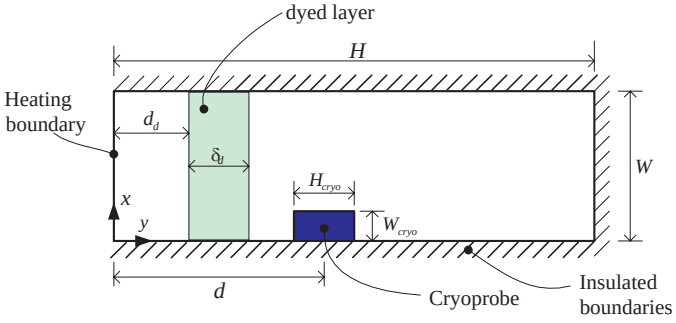

Figure 1. Schematic of computational domain.

To avoid undesirable heating damage, the irradiance of the laser is adjusted so the maximum temperature within the tissue is T_w. Concurrently, this allows us to compare under similar conditions the protecting effect of constant temperature heating *vs*. laser irradiation.

In order to determine how dyes may modify the temperature field within the tissue during laser irradiation, dye that changes the local attenuation coefficient to α_d is injected within the material at different depths, d_d. In order to keep the problem bounded, a single dyed layer thickness, δ_d, was used throughout the simulations.

The simulations are conducted under transient conditions. Initially, the tissue is at a temperature T_i. We are only concerned with protection of the tissue close to the surface by not allowing it to go below a lethal temperature, T_{lethal}. Since the displacement of the freezing front (and with it that of the T_{lethal} temperature contour) during the transient process is always toward the heating surface, the worst case scenario for tissue damage is when the steady state temperature is reached in the region of interest, which is when the freezing front gets closer to the heating boundary.

In order to assess the convenience of laser irradiation to protect a superficial layer of tissue, an effectiveness parameter, ε , is defined as the ratio of the thickness of the superficial layer of tissue above T_{lethal} obtained when laser irradiation is applied to the thickness of the superficial layer of tissue above T_{lethal} obtained when constant temperature heating is applied under similar physical and geometric conditions.

SIMULATION PARAMETERS AND PHYSICAL PROPERTIES

The geometric dimensions that were used in this investigation are the following: $H=8\times10^{-3}$m, $W=2.5\times10^{-3}$m, $H_{cryo}=1\times10^{-3}$m, $W_{cryo}=0.5\times10^{-3}$m, $\alpha_d=1\times10^{-3}$m, $2\times10^{-3}\text{m} < d < 7\times10^{-3}$m, and $1\times10^{-3}\text{m} \le d_d \le 3.5\times10^{-3}$m. The initial temperature of the tissue is T_i=37°C, which corresponds to the body temperature. The surface y=0 exchanges heat by convection (if specified) with a fluid at ambient temperature, T_∞=25°C, and the associated convective heat transfer coefficient is assumed to be h=150 Wm^{-2}K^{-1}, which is a characteristic value for free convection with a gas from a horizontal hot plate. Inserted inside the tissue is the cryoprobe that maintains a surface temperature of T_{cryo}=-145°C, characteristic of cryoprobes that use argon gas Joule-Thomson cooling effect [13]. The threshold for tissue thermal damage due to cryoinjury was set at T_{lethal}=-20°C, which is a value of temperature above which no permanent cryoinjury is expected [14]. The maximum temperature reached by the tissue for any of the two methods of heating, was fixed at T_w=50°C, this temperature is sufficiently high to produce heating from the wall, but not excessively high to induce thermal damage to the tissue.

The tissue is treated as a material having the properties of water or ice, depending on the temperature. Tissue is allowed to freeze at a temperature T_m=0°C, which is the pure water melt/freeze temperature at atmospheric pressure. The thermophysical properties of the tissue are considered to be temperature dependent, according to the following expressions, representing the water properties:

$$C=7.16(T+273)+138.0 \quad [\text{J kg}^{-1}\text{K}^{-1}] \quad T\le 0\,^\circ\text{C} \qquad (2a)$$

$$C=4186.8 \quad [\text{J kg}^{-1}\text{K}^{-1}] \quad T\ge 0\,^\circ\text{C} \qquad (2b)$$

$$k=2.24\text{-}5.975\times10^{-6}T^{1.156} \quad [\text{W m}^{-1}\text{K}^{-1}] \quad T\le 0\,^\circ\text{C} \qquad (3a)$$

$$k=0.1017+1.695\times10^{-3}(T+273) \quad [\text{W m}^{-1}\text{K}^{-1}] \quad T\ge 0\,^\circ\text{C} \qquad (3b)$$

$$\rho=920 \quad [\text{kg m}^{-3}] \quad T\le 0\,^\circ\text{C} \qquad (4a)$$

$$\rho=1000 \quad [\text{kg m}^{-3}] \quad T\ge 0\,^\circ\text{C} \qquad (4b)$$

and L=333730 J kg^{-1}.

The effective attenuation coefficient of the non dyed tissue was changed within $200 \le \alpha \le 1000$ m^{-1}. The attenuation coefficient of the dyed tissue was fixed at α_d=1500 m^{-1}.

MATHEMATICAL FORMULATION

The mathematical model that is presented below considers the tissue as a material that, because of its high water content, may be frozen when the temperature is below T_m. The heat balance equations that describe the heat transfer under phase change conditions, are broken into three equations: liquid phase, solid phase and the solid liquid/interface.

Liquid phase:

$$\nabla\cdot(k_l\nabla\cdot T)+Q=\rho_l C_l\frac{\partial T}{\partial t} \qquad T>T_m, \qquad (5)$$

Solid phase:

$$\nabla\cdot(k_s\nabla\cdot T)+Q=\rho_s C_s\frac{\partial T}{\partial t} \qquad T>T_m, \qquad (6)$$

where k is thermal conductivity, T temperature, Q an internal heat source term, ρ density, C specific heat and t time. The

subscripts *s* and *l* are used to indicate solid and liquid phases, while *m* is used to denote the melting front position.

At the solid/liquid interface:

$$k_l \frac{\partial T_l}{\partial \bar{n}} - k_s \frac{\partial T_s}{\partial \bar{n}} = \pm \rho_m L \frac{\partial \hat{\lambda}}{\partial t} \qquad T = T_m \,, \tag{7}$$

where $\bar{n}$ is the direction normal to the interface, L the latent heat, ρ_m is the mean density at the phase change temperature and $\hat{\lambda}$ is the interface location. The plus or minus sign in Equation (3) applies to solidification or melting, respectively.

The heat generation term in equations (5) and (6) comes from the laser irradiation to the tissue. If we assume that that the local rate of absorption of radiant energy is proportional to the intensity (i.e. Beer's absorption law), we arrive to the following expression for the heat source term

$$Q(y) = \alpha I_0 e^{-\alpha y}. \tag{8}$$

Other contributions to the heat generation term, such as metabolic heat generation and blood perfusion were also considered in the simulations but they appeared to have small influence on the temperature profile, especially considering the fact that freezing of the tissue cancels the possibility of blood irrigation to the tissue.

The set of equations stated before are better solved by the enthalpy method. In the enthalpy method, the only equation that needs to be solved is the integral heat balance over the volume and time-interval:

$$\int_t^{t+\Delta t} \frac{\partial}{\partial t}\left(\int_V E dV \right) dt = \int_t^{t+\Delta t} \int_{\partial V} -\vec{q} \cdot \vec{n} dS dt + \int_t^{t+\Delta t} \int_V Q dV dt, \tag{9}$$

where

$$E(x,y,t) = \begin{cases} \int_{T_m}^{T(x,y,t)} \rho_s C_s(\varphi) d\varphi & T(x,y,t) < T_m, \\ \int_{T_m}^{T(x,t)} \rho_l C_l(\varphi) d\varphi + \rho_m L & T(x,y,t) > T_m. \end{cases} \tag{10}$$

The scheme used here to solve the equations is based on the following explicit finite volume formulation:

$$E_{i,j}^{\,n+1} = E_{i,j}^{\,n} + \frac{\Delta t}{\Delta x}(q_{i-1/2,j} - q_{i+1/2,j}) + \frac{\Delta t}{\Delta y}(q_{i,j-1/2} - q_{i,j+1/2}) + \frac{\Delta t}{\Delta x}\int_{y_{j-1/2}}^{y_{j+1/2}} Q(y) dy \,. \tag{11}$$

RESULTS

The numerical code used in this investigation was validated by comparing it to benchmark results for the case of a square prism containing initially a liquid at a constant temperature, and exposed suddenly on its borders to a gas which flows at a temperature lower than the freezing temperature of the liquid. The associated convective heat transfer coefficient between the gas and the prism surface is *h*. As a result of the exposure to convection at this temperature, a freezing front moves toward the core of the square as time passes. The dimensionless parameters of the simulation are the following: Θ_i=9/7, where Θ =(T-T_∞)/(T_m-T_∞), *St*=2.0, where $St=C_s\,(T_m-T_\alpha)/L$, β=0.9, κ=k_l/k_s=0.9, and $Bi=hy_o/k_s$=2.0. Figure 2 shows the interface position as a function of time obtained by this simulation and a comparison with the results obtained by other two investigations [15-16]. The results are very similar to those of the other two authors, verifying the ability of this code to simulate the freezing process of a pure substance.

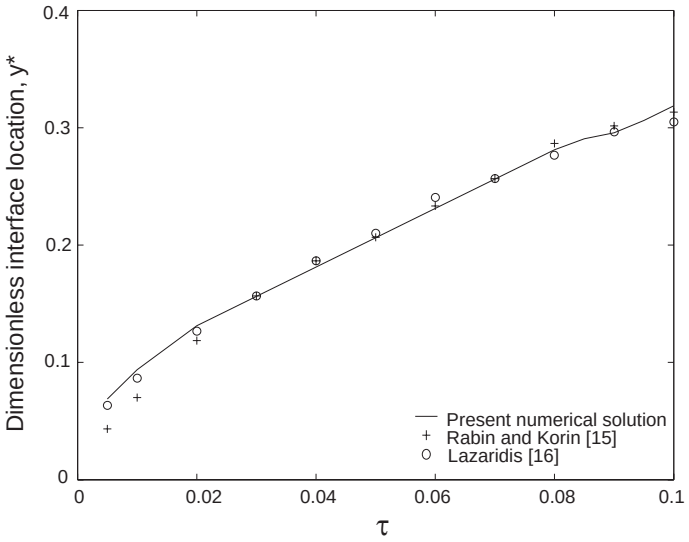

Figure 2. Validation of numerical code with square prism benchmark.

There are two clearly defined regions in the computational domain: *i*) the region between the heating surface and the cryoprobe and *ii*) the region between the cryoprobe and the surface $y=H$. Region *i*) quickly reaches steady state and region *ii*) evolves into steady state very slowly. The first region is the one in which we are interested in since that is the area to be protected by laser irradiation. All numerical simulations presented in this document are for the case t=250 s, time at which region *i*) has reached steady state and region *ii*) is evolving very slowly towards steady state.

The numerical simulations were performed in a mesh containing 20 by 64 divisions in the x any y directions, respectively. The time interval was restricted by the stability criterion that applies to explicit finite volume formulations. In order to study the independence of the results on the mesh size, a numerical simulation was run for a mesh containing 15 by 48 divisions in the x and y directions for the case $d=5\times10^{-3}$ m and α=500 m^{-1}; the difference in the final position of the -20°C temperature contour obtained for this mesh and the regular mesh was very small (less than 0.5%).

The application of the boundary condition at $y=H$ may have an effect on the temperature field obtained from the simulations. However, the region located between the cryoprobe and the irradiated surface is essentially unaffected by the value of H chosen for the computational domain. As a demonstration of the small effect that the dimension of H has on the temperature field between the cryoprobe and the

irradiated surface, the case $d=5\times10^{-3}$ m and $\alpha=500$ m^{-1} was simulated with two different computational domains: one where $H=0.008$ m and a second one where $H=0.024$ m; the difference in the final position of the -20°C temperature contour obtained for the two values of H was negligibly small (less than 0.1%).

Figure 3 shows the temperature contour that is obtained for the case of constant temperature heating, with the cryoprobe located at $d=5\times10^{-3}$m. As we can see from the figure, there is a steep temperature gradient near the surface, $y=0$. The constant temperature line T_{lethal}=-20°C is located at $y=0.8\times10^{-3}$m from the surface. Figure 4 shows the temperature contours obtained for the case of regulated laser heating with $\alpha=500$ m^{-1} and $d=5\times10^{-3}$m. In this case the constant temperature line T_{lethal}=-20°C has moved away from the surface to $y=1.6\times10^{-3}$m, increasing the thickness of protected tissue by $\varepsilon=2.0$ with respect to the constant temperature heating for the same set of parameters.

Figure 5 shows the comparison of temperature profiles, $T(W,y)$, of regulated laser heating *vs.* constant temperature heating for two different cryoprobe positions. The greatest effectiveness of regulated laser irradiation protection occurs when the cryoprobe is located nearest to the surface, at $d=3\times10^{-3}$m, case for which the effectiveness coefficient is $\varepsilon=2.858$. For the case of the deepest cryoprobe, $d=7\times10^{-3}$m, the effectiveness coefficient is $\varepsilon=2.07$. Figure 5 illustrates that the use of laser heating has a potential for use in protection during cryosurgery, especially when the dimensions involved in the cryoprocedure are small.

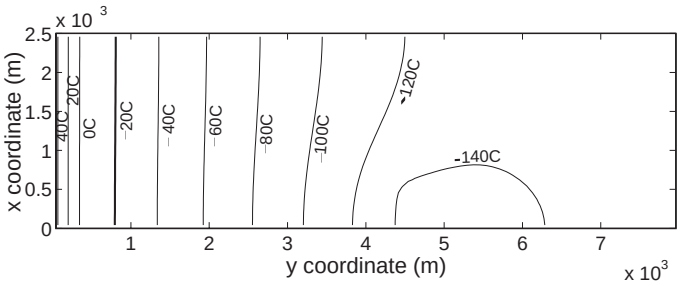

Figure 3. Temperature contours for constant temperature heating of tissue. $d=5\times10^{-3}$m.

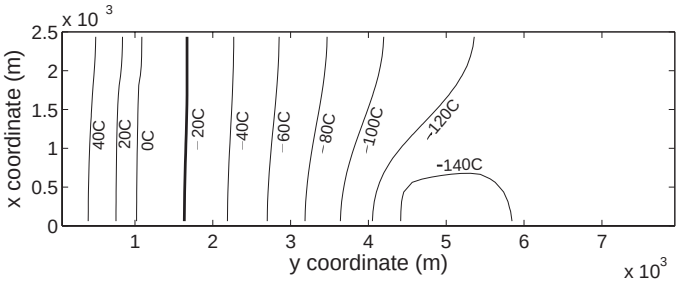

Figure 4. Temperature contours for regulated laser irradiation of tissue $d=5\times10^{-3}$m, $\alpha=500$m^{-1}.

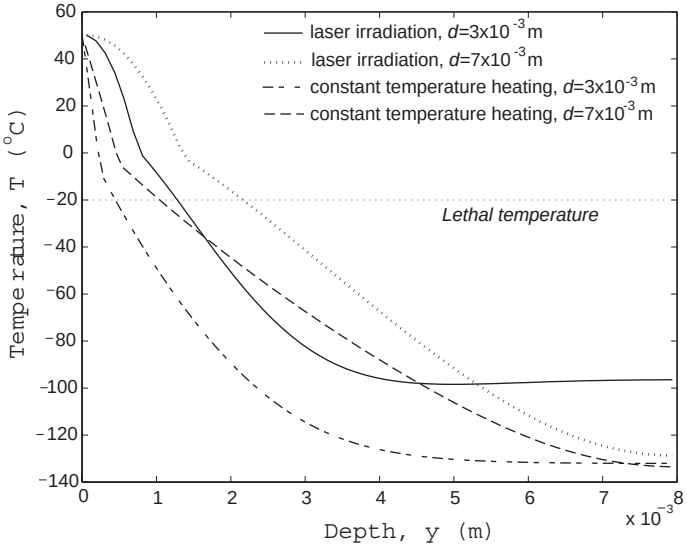

Figure 5. Temperature as a function of depth, $T(W,y)$, for $\alpha=500$ m^{-1} and three different values of d. Regulated laser *vs.* constant temperature heating.

The characteristics of the laser and the tissue are determinant to appraise the convenience of laser irradiation as a means of protection of a layer of tissue. The optical parameter that is critical is the attenuation coefficient, α, since it determines the distribution of absorbed energy as a function of depth. Figure 6 shows the influence that α has on the temperature profile $T(W,y)$ for a given position of the cryoprobe. For the largest value of the attenuation coefficient used in this study, $\alpha=1000$ m^{-1}, most of the laser energy is absorbed near the surface and the protection attained by laser heating is still effective, but inferior to the other cases of smaller attenuation coefficients. In the cases $\alpha=200$ m^{-1} and $\alpha=250$ m^{-1}, the energy is absorbed more uniformly over the thickness of the layer, and a rebound on the temperature profile is observed deep in the tissue at locations far from the cryoprobe position. This is interesting because, under the assumption of a uniform attenuation coefficient, two different regions of protected tissue may be attained. For the case $\alpha=200$ m^{-1} and $d=3\times10^{-3}$m, these regions are the superficial region, $y\leq 1.58\times10^{-3}$ m, and the deep region, $y\geq 5.46\times10^{-3}$ m.

The injection of a dye at a certain tissue depth produces the extra benefit of absorbing most of the laser energy at selected regions inside the tissue, and this may serve to displace the lethal temperature contour to a deeper position from the surface. Figure 7 shows temperature contours of the tissue if a layer of dye that modifies the attenuation coefficient of the tissue to $\alpha_d=1500$ m^{-1} is injected at 2.5×10^{-3} m < d < 3.5×10^{-3} m; compared with Figure 2, the contour plot is modified by further displacing the temperature line T_{lethal}=-20°C away from the surface to a position $y\approx2.5\times10^{-3}$m, representing an increase in thickness of protected tissue of $\varepsilon=3.125$.

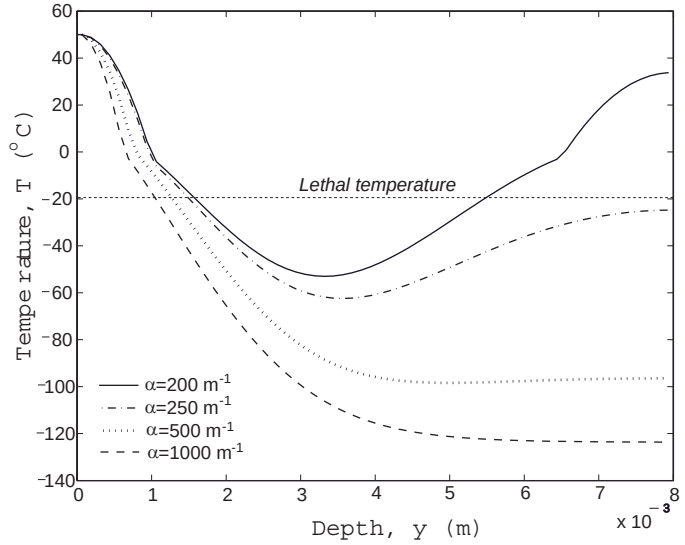

Figure 6. Temperature as a function of depth, $T(W,y)$, for $d=3\times10^{-3}$m and three different values of α.

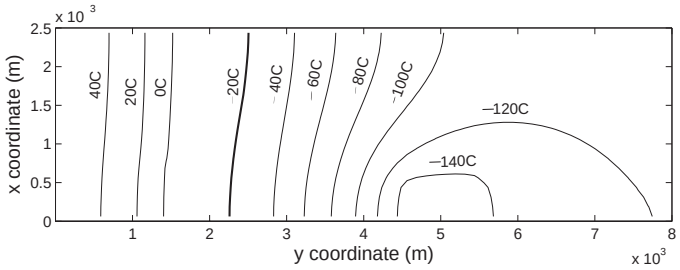

Figure 7. Temperature contours for regulated laser heating of tissue. $d=5\times10^{-3}$m, α=500 m^{-1}. Dye with α_d=1500 m^{-1} was injected at 2.5×10^{-3} m < y < 3.5×10^{-3} m.

The place where the dye is injected determines, to some extent, the temperature profile that is obtained. In order to increase the layer of tissue that is protected from lethal damage, the dye has to be placed at an optimum depth from the surface. If the dye is placed too close to the surface it will produce absorption of energy close to the surface, restricting the amount of regulated laser energy, and moving the lethal temperature line closer to the surface. If the dye is injected very far from the surface, it will not produce any benefit with respect to the undyed tissue, as much of the laser energy would have already been absorbed by the tissue above this layer. Figure 8 shows the temperature profiles, $T(W,y)$, that are obtained when dye is injected at a given depth. It is possible to see how the thickness of protected tissue varies as a function of depth of dyed tissue. The results suggest that there is an optimum placement of the dye within the tissue that produces the highest superficial protection to the tissue, and that the thickness of dyed tissue is also relevant.

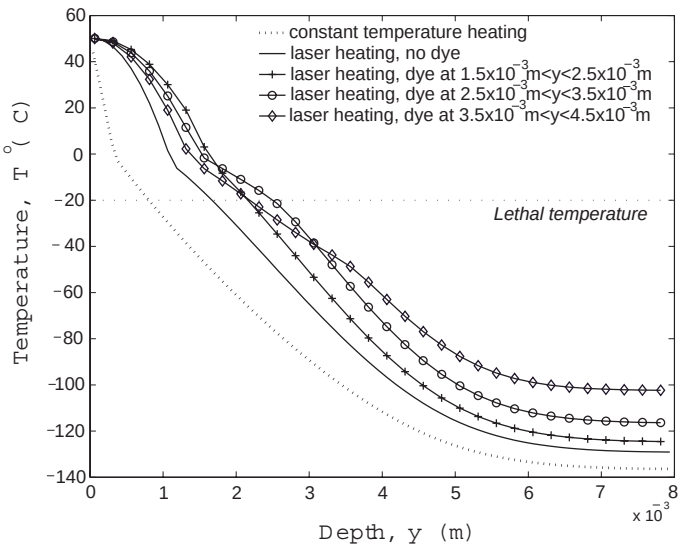

Figure 8. Temperature as a function of depth, $T(W,y)$, for α=500 m^{-1}, $d=5\times10^{-3}$m. Comparison of constant temperature heating, laser heating without dye and three different depths of dye injection with α_d=1500 m^{-1}.

CONCLUSIONS

The investigation presented herein explores the convenience of laser irradiation heating for the purpose of freezing front confinement and to limit the damage produced by exposing the tissue to temperatures below the lethal threshold. For this purpose, a numerical simulation is performed, and the worst case scenario of thermal damage is computed for steady state conditions in the region that needs to be protected. The differences in thermal confinement produced by the conventional constant temperature heating technique and regulated laser irradiation heating are assessed. The results confirm the superiority of laser irradiation as a means of protection of a superficial layer of tissue: in all cases evaluated, the use of regulated laser heating protects a much thicker layer of tissue than the conventional constant temperature heating. The best protection occurs when the cooling device (cryoprobe) is placed near the surface, when the attenuation coefficient of the material is low, and when dyes are injected into the tissue to promote localized absorption of laser irradiated energy. In the case of dye injection into the tissue, the placement of the dye results in an optimization problem, in which the thickness of the dye layer as well as its placement within the tissue are parameters that should be varied to maximize the superficial tissue protection.

ACKNOWLEDGMENTS

The authors would like to acknowledge the support of UC MEXUS program for a Faculty Fellowship granted to R. Romero-Méndez to spend a sabbatical year at UCR.

REFERENCES

[1] Arnott J., 1851, The treatment of cancer through the regulated application of an anaesthetic temperature. J&A Churchill, London.

[2] Cooper I.S. and Lee A., 1961, Cryostatic congelation: a system for producing a limited controlled region of cooling or freezing of biological tissue, Journal of Nervous Mental Disorders, **133**, pp 259-269.

[3] Onik G.M., Cohen J.K., Reyes G.D., Rubinsky B., Chang Z.H., and Baust J, 1993, Transrectal ultrasound-guided percutaneous radical cryosurgical ablation of the prostate, Cancer, **72**, pp. 1291-1299.

[4] Chang Z., Finkelstein J.J., Ma H., and Baust J., 1994, Development of a high-performance multiprobe cryosurgical device, Biomedical Instrumentation Technology, **28**, pp. 383-390.

[5] Rabin Y., and Shitzer A., A new cryosurgical device for controlled freezing, Part I: setup and validation test, Cryobiology, **33**, pp. 82-92.

[6] Rabin Y., Coleman R., Mordohovich D., Ber R., and Shitzer A., 1996, A new cryosurgical device for controlled freezing, Part II: in vivo experiments on rabbits' hind thighs, Cryobiology, **33**, pp. 93-105.

[7] Cohen T.K., Miller R.J., and Shumarz B.A., 1995, Urethral warmer catheter for use during cryoablation or the prostate, Urology, **45**, pp. 861-864.

[8] Mala T., Aurdal L., Frich L., Samset E., Hol P.K., Edwin B., Soreide O. and Gladhaug I., 2004, Liver Tumor Cryoablation: a commentary on the need of improved procedural monitoring, Technology in cancer research and treatment, 3, pp. 85-91.

[9] Baissalov R., Sandison G.A., Reynolds D. and Muldrew K., Simultaneous optimization of cryoprobe placement and thermal protocol for cryosurgery, Physics in Medicine and Biology, **46**, pp. 1799-1814.

[10] Rewcastle J.C., Sandison G.A., Muldrew K., Saliken J.C. and Donnelly B.J., 2001, A model for the time dependent three-dimensional thermal distribution within iceballs surrounding multiple cryoprobes, Medical Physics, **28**, pp. 1125-1137.

[11] Rabin Y., Lung D.C., and Stahovich T.F., 2004, Computerized planning of cryosurgery using cryoprobes and cryoheaters, Technology in Cancer Research and Treatment, **3**, pp. 229-243.

[12] Rabin Y. and Stahovich T.F., 2002, The thermal effect of urethral warming during cryosurgery, CryoLetters, **23**, pp. 361-374.

[13] Rabin Y. and Stahovich T.F., 2003, Cryoheater as a means of cryosurgery control, Physiscs in Medicine and Biology, **48**, pp. 619-632.

[14] Hoffmann N.E. and Bischof J.C., 2002, The cryobiology of cryosurgical injury, Urology, 60, pp. 40-49.

[15] Rabin Y. and Korin E., An efficient numerical solution for the multidimensional solidification (or melting) problem using a microcomputer, International Journal of Heat and Mass Transfer, **36**, pp. 673-683.

[16] Lazaridis A., A numerical solution of the multi-dimensional solidification (or melting) problem, International Journal of Heat and Mass Transfer, **13**, pp. 1459-1477.